



Deposited via The University of Leeds.

White Rose Research Online URL for this paper:

<https://eprints.whiterose.ac.uk/id/eprint/133969/>

Version: Accepted Version

Article:

Ladd-Parada, M, Povey, MJ, Vieira, J et al. (2019) Fast Field Cycling NMR relaxometry studies of molten and cooled cocoa butter. *Molecular Physics*, 117 (7-8). pp. 1020-1027. ISSN: 0026-8976

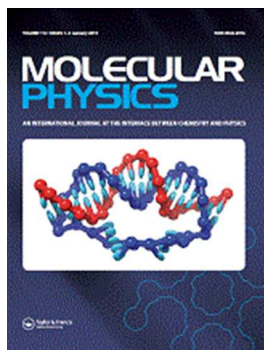
<https://doi.org/10.1080/00268976.2018.1508784>

Reuse

Items deposited in White Rose Research Online are protected by copyright, with all rights reserved unless indicated otherwise. They may be downloaded and/or printed for private study, or other acts as permitted by national copyright laws. The publisher or other rights holders may allow further reproduction and re-use of the full text version. This is indicated by the licence information on the White Rose Research Online record for the item.

Takedown

If you consider content in White Rose Research Online to be in breach of UK law, please notify us by emailing eprints@whiterose.ac.uk including the URL of the record and the reason for the withdrawal request.



Fast Field Cycling NMR relaxometry studies of molten and cooled cocoa butter

Journal:	<i>Molecular Physics</i>
Manuscript ID	Draft
Manuscript Type:	Special Issue Paper
Date Submitted by the Author:	n/a
Complete List of Authors:	Ladd Parada, Marjorie; University of Leeds, School of Food Science and Nutrition Povey, Malcolm; University of Leeds, School of Food Science and Nutrition Vieira, Josélio; Nestle Product Technology Centre York Ries, Michael; University of Leeds, School of Physics and Astronomy
Keywords:	cocoa butter, triacylglycerols, diffusion, FFC-NMR

SCHOLARONE™
Manuscripts

1
2
3 **Fast Field Cycling NMR Relaxometry Studies of Molten and Cooled**
4 **Cocoa Butter**
5

6
7 Marjorie Ladd Parada^{a*}, Malcolm J.W. Povey^a, Josélio Vieira^b, and
8 Michael E. Ries^c
9

10
11
12 ^a *School of Food Science and Nutrition, University of Leeds, LS2 9 JT, Leeds, U.K.*
13

14 ^b *Nestlé, Product Technology Centre, York, U.K.*
15

16
17 ^c *School of Physics and Astronomy, University of Leeds, LS2 9 JT, Leeds, U.K.*
18
19

20
21
22 *Corresponding author: Marjorie Ladd Parada, School of Food Science and Nutrition,
23 University of Leeds, LS2 9 JT, Leeds, U.K., e-mail: marladdp@gmail.com
24
25
26
27
28
29
30
31
32
33
34
35
36
37
38
39
40
41
42
43
44
45
46
47
48
49
50
51
52
53
54
55
56
57
58
59
60

Fast Field Cycling NMR Relaxometry Studies of Liquid and Cooled Cocoa Butter

Due to its relevance in the confectionery industry, cocoa butter (CB) has been extensively studied. However, most studies focus on its crystallisation properties, whilst studies of its liquid state are lacking. Here, and for the first time, a study of the self-diffusion of CB at different temperatures is presented, using fast field cycling (FFC) nuclear magnetic resonance (NMR) further validated using pulsed field gradient stimulated echo (PGSTE) NMR. Measurements were performed upon heating CB to either 50 or 100 °C and cooling it to 22 °C. No hysteresis was found between the different thermal treatments. However, the activation energy (28.7 kJ/mol) estimated from the cooling protocol of the 100 °C treatment, was the closest to that reported in literature for similar systems. This suggests that measurements using a wider range of temperatures, and starting with a liquid material are advisable. Additionally, samples were measured during isothermal crystallisation at 22 °C, showing that the region below 1 MHz is the most sensitive to phase changes.

Keywords: cocoa butter, triacylglycerols, diffusion, FFC-NMR

Introduction

Cocoa butter (CB) is one of the most important confectionery fats as it is responsible for the key sensory characteristics and stability of chocolate[1]. However, this is only possible when CB is present in a specific crystal form, namely the β -V phase[1-3]. Hence, most studies have focused on CB's solid structure[4-12]. Nevertheless, the understanding of CB's liquid phase is relevant, as it might hold information on what happens prior to crystallisation, such as the pre-nucleating structures proposed by previous authors for other fats[13-18]. In addition, information regarding the liquidity of the fatty acid (FA) chains in the triacylglycerols (TAGs) comprising the fat in the solid state is relevant to solid state phase transitions, such as from the β' -phase to the β -phase.

1
2
3 This is because a displacement and rearrangement of the TAG molecules is required for
4
5 the generation of new lamellar and sub-cell structures, as well as the perfecting of the
6
7 crystals[19-22].
8

9
10 Studies in liquid fats have previously focused on X-ray or neutron scattering
11
12 measurements[14, 15, 23]; however, self-diffusion studies of pure triacylglycerols
13
14 (TAGs) have also been performed[24-27]. Only two of these studies determined self-
15
16 diffusion experimentally, whilst the other two are computer simulation predictions.
17
18 Interestingly, the two experimentally-based studies use different methodologies,
19
20 Callaghan *et al.*[24] used the standard pulse gradient stimulated echo sequence
21
22 (PGSTE) [28, 29], and Rachocki and Tritt-Goc[27] used FFC-NMR. This technique,
23
24 thanks to the advances in the area, has become more readily accessible, and has been
25
26 used more frequently for the study of viscous liquids such as polyols and polymers[30-
27
28 33].
29

30
31 It is therefore evident that self-diffusion measurements are sparse in the studies
32
33 of fats and oils. More specifically, to the best of our knowledge, no self-diffusion
34
35 measurements in liquid CB have been reported up to date using either of the NMR
36
37 techniques. Therefore, the main objective of this paper was to measure the self-diffusion
38
39 of CB using both, PGSTE and FFC-NMR, making it the first study of its kind.
40

41
42 Finally, whilst FFC-NMR has been mainly applied for the evaluation of liquid
43
44 systems, it has also been observed useful in the studies of solid state matter, including
45
46 crystal systems[34, 35]. Furthermore, NMR is a staple technique in the oil and fat
47
48 industry for the determination of the solid fat content (SFC), allowing for the study of
49
50 crystallisation kinetics[36, 37]. Thus, as secondary objective, the applicability of FFC-
51
52 NMR for crystallisation studies was evaluated.
53
54
55
56
57
58
59
60

Materials and Methods

Refined, bleached and deodorised West-African CB was used in all experiments without any further refinement.

FFC-NMR Diffusion measurements

Glass NMR tubes of 0.8 mm inner diameter were filled with approximately 2.5 cm of molten CB (50 °C), which was then left at ambient temperature for two weeks to allow for crystallisation prior to measurements. ^1H NMRD profiles were obtained on a Stelar SMARtracer FFC NMR Relaxometer (Stelar s.r.l., Mede, PV, Italy).

Samples were heated from 22 °C to 25, 27, 30, 35, 37 and 40 °C and subsequently to either 50 or 110 °C in 10 °C steps, allowing 10 min for thermal equilibration at each temperature. Samples were subsequently cooled to 22 °C, following a reversed protocol in cooling direction allowing for an equilibration time of 15 min. Once 22 °C was reached, the samples were held isothermally for 120 min and measured continuously. Each full relaxation dispersion measurement took approximately 6 minutes, thus, the first measurement performed at 10 MHz corresponds to 1 min of isothermal time, whilst the first measurement made at 0.01 MHz corresponds to 6 min of isothermal time.

The proton spins were submitted to a polarisation field of 7 MHz for a period of about five times the T_1 estimated at this frequency. Afterwards, the magnetic field was switched to the corresponding relaxation field between 0.01–10.0 MHz. FIDs were recorded following a single ^1H 90° pulse applied at 7 MHz. Field-switching time was 2.5 ms, while the spectrometer dead time was 15 to 20 μs . A recycle delay of 5 T_1 was always used. A non-polarized FFC sequence was applied at relaxation fields of 10.0–1.6 MHz, whilst a polarized FFC sequence was applied at fields below 1.6 MHz.

Diffusion coefficients were calculated from the obtained R_1 values following the methodology proposed by Kruk, Meier and Rössler [38]

$$R_1(\nu) \cong R_1(0) - B\sqrt{\nu} = R_1(0) - N \left(\frac{\mu_0}{4\pi} \gamma_H^2 \hbar \right)^2 \left(\frac{\sqrt{2+8}}{30} \right) \left(\frac{\pi}{D} \right)^{\frac{3}{2}} \sqrt{\nu} \quad (1)$$

where B was estimated from the slope of the R_1 vs frequency curve, ν is the frequency, N the number of nuclei per cubic metre (in this case hydrogen), μ_0 is the permeability of free space, γ_H is the gyromagnetic factor of hydrogen, \hbar is the reduced Planck's constant, and D is the self-diffusion coefficient. Given that CB is primarily composed by a mix of TAGs, N was estimated from

$$N = \rho n / M \quad (2)$$

where ρ is the density, n is the average number of hydrogens per molecule and M the average molar mass, where both n and M were calculated as an average of the values of the three main TAGs in CB, density was measured in a DMA 4500 vibrational density meter (Anton Paar, GmbH, Graz, Austria).

Finally, all diffusion coefficients were plotted against temperature and fitted according to the linearized version of the Arrhenius equation[39]

$$\ln D = \ln D_0 - \frac{E_a}{RT} \quad (3)$$

where D_0 is the pre-exponential factor (m^2/s), which is independent of temperature, E_a is the activation energy, and R is the ideal gas constant.

Data was also fitted to the Vogel-Fulcher-Tammann (VFT) equation

$$\ln D = \ln D_0 - \frac{B}{(T-T_0)} \quad (4)$$

where D_0 is the pre-exponential factor (m^2/s), B is a material dependent parameter that

can be associated to the activation energy, and T_0 is usually interpreted as the ideal glass transition or crystallisation temperature[40, 41].

PGSTE-NMR measurements

For temperatures below 50 °C, 5 mm glass NMR tubes were filled with approximately 1 cm of molten CB (50 °C) and left to crystallise for at least a week at ambient temperature. For treatments above 50 °C, a glass capillary of 2 mm inner diameter was filled with 0.5 cm of molten CB. This capillary was sealed and inserted in a 5 mm glass NMR tube. This set-up was necessary to reduce convection which causes an over-estimation of the diffusion coefficient[42, 43].

Self-diffusion coefficients were measured on a Bruker Avance II 400 MHz with a diffusion probe (Diff50). The diffusion time, Δ , was 60 ms, and the pulse gradient duration, δ , was 4 ms for all measurements. Measurements were taken at 35, 37, 40, 50, 60 and 70 °C. The samples were left to equilibrate for 10 min prior to measurements. Temperature was controlled with an accuracy of ± 0.1 °C.

The signal attenuation as a function of gradient was fitted using the Stejskal-Tanner equation[44-47],

$$S_g = S_0 e^{-D\gamma^2 g^2 \delta^2 (\Delta - \frac{\delta}{3})} \quad (7)$$

where S_g represents the signal as affected by diffusion, S_0 the initial signal, D the diffusion coefficient, and γ the gyromagnetic ratio of hydrogen. Diffusion coefficients were determined from the signal intensity measured as the area of the strongest peak in the spectrum, i.e. the one corresponding to the CH₂ groups within the FA chain.

Results and discussion

Diffusion coefficients calculated from PGSTE-NMR and FFC-NMR measurements

In the last decade, the use of FFC-NMR for the determination of self-diffusion has increased[30-32, 48]. Nevertheless, PGSTE-NMR remains the standard technique for this purpose[29, 49]. Therefore, the diffusion coefficients determined by FFC-NMR were validated using the latter, as shown in Figure 1.

From the previous figure, it is possible to see that the diffusion coefficients obtained by both methodologies are in good agreement with each other, as well as those taken from literature[24], and so are in agreement with the findings of Rachocki and Tritt-Goc[27]. In addition, it is noted that FFC-NMR has two main advantages over the PGSTE sequence. Firstly, no special set-up (small capillary inside the NMR tube) was required for measurements above 50 °C to avoid errors coming from convection effects. Secondly, temperatures of up to 100 °C were possible, whereas only temperatures of 70 °C were achievable with the current Bruker set-up. Hence making FFC-NMR an ideal method for diffusion measurements not only of vegetable oils, as shown by Rachocki and Tritt-Goc[27], but also of vegetable fats, like CB, which have a higher melting point.

Once the validity of the FFC-NMR measurements was ascertained, it was possible to evaluate the temperature dependence of self-diffusion, and the effect of the different maximum temperatures.

Temperature dependence of diffusion of cocoa butter

Comparing the different treatments, it is possible to observe that there was no hysteresis between the cooling and heating protocols (Figure 2A and B), nor between the two

1
2
3 maximum temperature treatments, 50 or 110 °C (Figure 3). This lack of hysteresis
4 indicates that whilst changes in microviscosity of TAG systems have been reported by
5 previous authors[50], they are not observable by bulk self-diffusion measurements,
6 suggesting they only occur in localised areas, probably near the ends of the FA side
7 chains or in the areas surrounding newly formed nuclei. It is noted, however, that
8 there is a difference in the diffusion coefficients measured at 70 °C (Figure 2B). It is
9 tempting to associate this behaviour with a phase transition as it coincides with the
10 melting point of tristearin[51-53], which is one of the minor components in CB.
11
12 Regardless, given that at lower temperatures the diffusion coefficients do not deviate
13 from those of the heating protocol, it is likely that this point is only an outlier.
14
15

16
17 As mentioned earlier, two different functions were fitted to the diffusion
18 coefficients, namely, the linearized Arrhenius equation (Figure 3) and the VFT model.
19 From Figure 4 it can be observed that the best fit is obtained by the latter. This lack of
20 linear trend is in agreement with the work from Greiner et al.[26], where the
21 temperature dependence of self-diffusion of fully saturated TAGs was simulated, but
22 contrasts with the linearity reported by Callaghan and Jolley[24]. However, it is
23 important to note that this could not be confirmed from the published plot, as the scale
24 used in both axes is variable, being neither linear nor logarithmic.
25
26

27
28 Even though the temperature dependence was better described by the VFT
29 function, from the Arrhenius fittings the E_a and D_0 could still be obtained (Table 1).
30 Here, it is evident that the D_0 s estimated from the 50 °C treatments are two to three
31 orders of magnitude larger than those reported in literature[24], whilst the 100 °C
32 treatments led to comparable values. This is easily explainable by the diffusion
33 coefficient having a change (decrease) of slope after reaching 60-70 °C (Figure 4). Thus
34 indicating that, by using 50 °C as maximum temperature, it is not possible to obtain a
35
36
37
38
39
40
41
42
43
44
45
46
47
48
49
50
51
52
53
54
55
56
57
58
59
60

full description of the temperature dependence, and that structural changes still occur above this temperature. This is likely due to the presence of crystalline material up to at least 70 °C because of the higher melting components of CB such as tripalmitin and tristearin[12, 54, 55]. Moreover, the D_0 calculated from the heating ramps is one degree of magnitude smaller than that estimated from the cooling ramps, whereas the E_a is larger, regardless of the maximum temperature. This is explained by the Arrhenius function not being able to predict the sharper slope describing the diffusion coefficients at lower temperatures (< 35 °C).

Table 1 Parameters of the VFT and Arrhenius equations fitted to the four different thermal treatments.

Fitted Parameter	Heating 35-50 °C	Cooling 50-22 °C	Heating 35-100 °C	Cooling 100-22 °C	StStSt[24]	OOO[24]
D_0 (10^{-10} m ² s ⁻¹) (VFT)	7.0±0.6	6.5±0.7	3.6±0.9	5.9±0.5	---	---
B (A.U.)	294.91±7.3	289.98±7.5	200.132±8.5	299.61±7.1	---	---
T_0 (°C)	-38.2±7.6	-39.0±2.9	-25.5±1.0	-31.80±1.9	---	---
D_0 (10^{-6} m ² s ⁻¹) (Arrhenius)	31.8±0.02	200.0±5.4	0.30±0.01	1.04±0.02	0.47±0.09	0.93±0.07
E_a (kJ/mol)	35.6±0.7	43.3±0.9	25.4±0.5	28.7±0.6	27.0±0.1	28.1±0.5

Furthermore, the estimated D_0 and E_a are closer to those reported for triolein[24] (Table 1). This is thought to be caused by the presence of an oleoyl chain in most of the TAGs present in CB. This oleoyl chain is known to decrease the melting temperature considerably (73 °C of tristearin[56] vs. 44 °C of StOSt[57]), and consequently, the energy required for any structural changes. This effect has been related to the oleoyl chain having an increased rotational freedom at the double bond, combined with increased entropy due to the steric hindrance between the bent oleoyl chain and the straight methyl chain of the saturated FAs[58, 59]. This is in contrast with the diffusion coefficient at 70 °C being closer to the value of tristearin (Figure 1). Nevertheless, it must be taken into consideration that whilst the oleoyl chains might be the drivers for the start of diffusion at lower temperatures, at 70 °C it is the saturated FAs that are

1
2
3 expected to govern the changes in diffusion, particularly when forming part of the fully
4 saturated TAG molecules. This is related, once more, to their having melting points
5 above 60 °C[56, 60].
6
7

8
9 Regarding the VFT derived parameters, it is evident that the estimated D_0 s are
10 considerably lower than those determined from the Arrhenius fittings (Table 1). This is
11 unsurprising as the Arrhenius function does not take into consideration the decreased
12 slope at higher temperatures, thus overestimating the values of D_0 . Regardless, the D_0 s
13 from the 100 °C treatment showed a similar trend to that of the Arrhenius fitting, the
14 values estimated from the heating ramp were smaller compared to those estimated from
15 the VFT. Contrastingly, no difference was observable between any of the parameters
16 derived from the heating and cooling ramps of the 50 °C treatment. Given that the VFT
17 curve does describe the changes in slope, it can predict the increase of slope at
18 temperatures below 35 °C. In contrast, in the 100 °C treatment, when these values are
19 lacking, the smaller slope observed from 60 °C onwards skews the fit towards higher
20 diffusion factors. Thus reinforcing the need of applying the right function and of using a
21 wide range of temperatures.
22
23
24
25
26
27
28
29
30
31
32
33
34
35
36

37 From the VFT fittings, an additional parameter was obtained, the T_0 , which is
38 commonly associated with glass or crystallisation transitions[39]. Surprisingly, even
39 though CB is usually observed to crystallise at temperatures above 10 °C[61], all
40 estimated T_0 s were below zero degrees (-40 to -25 °C). Nevertheless, a metastable form
41 has been previously reported when cooling CB to temperatures between -30 and 5 °C
42 [4, 5, 61]. Thus, these T_0 s could be related to the crystallisation of this specific crystal
43 form, although a glass transition cannot be disregarded at this stage. Further studies are
44 required to determine the origin of such very low temperature values.
45
46
47
48
49
50
51
52
53
54
55
56
57
58
59
60

Isothermal relaxometry measurements of cocoa butter

FFC-NMR relaxometry measurements were continued for two hours after reaching 22 °C to evaluate the feasibility of using this methodology not only for the study of CB in the liquid phase, but also during the crystallisation process. These studies were prompted by the FID T_1 measurements commonly used for the determination of the percentage of solids in crystallising fat[36], and previous reports on the applicability of FFC-NMR measurements for the study of crystalline materials[34, 35].

From Figure 5, it is possible to see that the R_1 values in the region between 0.01 and 0.63 MHz increase over time, particularly in the 50 °C treatment. This increase in R_1 is expected upon solidification of the material, thus confirming that FFC-NMR is sensitive to the progression of CB crystallisation. Based on the previous, it is possible to assume that by heating CB to 100 °C crystallisation is reduced, as the R_1 only reached values of approximately 40 s⁻¹, whereas in the 50 °C treatment, values above 100 s⁻¹ were observed at 0.01 MHz after two hours. This could be related to the 50 °C treatment retaining a small amount of crystal clusters from the higher melting TAG species present in CB, which then serve as heterogeneous nuclei[10, 52, 62]. Contrastingly, at 100 °C, these small crystalline structures are expected to have become fully molten, thus delaying crystallisation.

It is noted that, whilst FFC-NMR has the potential of being used for crystallisation measurements, it is not thought to be a substitute for the current SFC technique[37, 63], simply because of measuring times. As mentioned earlier, a single FFC-NMR measurement takes approximately 6 min, whereas an SFC measurement takes less than a minute. This makes the latter ideal for tracking the initial stages of crystallisation, especially in cases where crystallisation occurs within the first 30 min of the isothermal period, as in the case of the 50 °C treatment. Regardless, in-depth

1
2
3 analysis of the FFC-NMR dispersion curves, by covering a range of frequencies, has the
4
5 potential of providing information on different types of molecular motion, as well as the
6
7 degree of ordering that occur over time, i.e. information both on the remaining liquid
8
9 and the solid forming, similarly to what has been applied for the studies of liquid
10
11 crystals[64-66].
12

13
14 Finally, it is interesting to note that the spectral density above 1 MHz contains
15
16 little information about the crystallisation and dynamics in these systems, highlighting
17
18 the importance of exploring a range of frequencies, and showing that the lower range
19
20 (below 1 MHz) is more sensitive to these systems, thus providing complementary
21
22 information to that obtained at the 20 MHz used for SFC.
23
24

25 26 **Conclusions**

27
28 Self-diffusion measurements of CB are presented, for the first time, using two
29
30 methodologies, the standard PGSTE method and FFC-NMR. This comparison validates
31
32 the latter as a good alternative method for diffusion measurements. Moreover, FFC-
33
34 NMR measurements have proved to be better suited for the studies of fats, as no special
35
36 set-up was required to prevent convection errors, as was the case for the standard
37
38 PGSTE-NMR measurements, and provided more ready access to a wider temperature
39
40 range.
41
42

43
44 Additionally, whilst no hysteresis was observed in the diffusion coefficients
45
46 obtained from any of the four different treatments, different fitting parameters were
47
48 obtained. Interestingly, the D_0 and E_a estimated from the cooling curve of the 100 °C
49
50 treatment were closer to the ones reported in literature, particularly those of triolein,
51
52 whilst the diffusion coefficient at 70 °C is closer to that of tristearin. This highlights the
53
54 importance of using a wide range of temperatures as well as the relevance of starting
55
56 with a fully molten material. More importantly, though, it evidences oleoyl chains
57
58
59

1
2 driving the start of diffusion because of their higher mobility, and thus the activation
3 energy, in systems composed of mixed TAGs (with unsaturated and saturated FAs).
4
5 Nonetheless, as temperature increases, it is the saturated FAs which are expected to
6
7 have a stronger influence. Further studies are suggested, using ^{13}C NMR, to confirm this
8
9 hypothesis.
10
11

12
13 Regarding the isothermal measurements, it is concluded that FFC-NMR is suited
14
15 to following crystallisation in fats, even if not in a time resolved fashion. Importantly,
16
17 the most sensitive region to structural changes upon solidification was that below
18
19 1 MHz. Hence, further analysis of the dispersion curves is recommended to determine
20
21 the contribution of different molecular motions and evaluate the changes through time.
22
23 This could provide insights into the initial stages of crystallisation, particularly when
24
25 slow crystallisation kinetics are observable. As an ancillary technique, X-ray scattering
26
27 studies would allow the detection of the development of different crystalline forms, thus
28
29 helping to determine if different polymorphs can also be identified using FFC-NMR,
30
31 similarly to T_l measurements at 60 MHz[60]. This would prove particularly helpful, as
32
33 the mechanism of polymorphic transformations between the different polymorphs could
34
35 be explored in further detail.
36
37
38
39
40

41 **Graphical abstract**

42
43
44
45
46

47 **Funding details**

48
49 This work was funded by the Consejo Nacional de Ciencia y Tecnología (México) in
50
51 the form of a full scholarship for the PhD studies of Marjorie Ladd Parada.
52
53

54 Nestlé, Product Technology Centre, York, provided the cocoa butter used in this study,
55
56
57
58
59

and Nestlé, Ltd provided financial support for Marjorie Ladd Parada's PhD project.

Acknowledgements

The authors would like to thank Dr Daniel Baker, from the University of Leeds, who helped with the set-up of both the PGSTE-NMR and the FFC-NMR. The experiments in the latter were made possible by the NMR Small Research Facility in the School of Physics and Astronomy of the University of Leeds. M.E.R. is a Royal Society Industry Fellow.

The authors would also like to thank COST ACTION CA15209 who gave financial aid to Marjorie Ladd Parada for her attendance to the Training School [NMR relaxometry for food and environmental applications].

Disclosure statement

No potential conflict of interest is reported by the authors.

References

- [1].S. T. Beckett, in *Science and Technology of Enrobed and Filled Chocolate, Confectionery and Bakery Products*, edited by G. Talbot (Woodhead Publishing, 2009), pp. 11.
- [2].S. T. Beckett, *Science of Chocolate*. (The Royal Society of Chemistry, United Kingdom, 2000).
- [3].E. J. Windhab, in *Industrial Chocolate Manufacture and Use*, edited by S. T. Beckett (Wiley-Blackwell, United Kingdom, 2007), pp. 276.
- [4].R. L. Wille and E. S. Lutton, *Journal of the American Oil Chemists Society* **43** (8), 491 (1966).
- [5].G. M. Chapman, E. E. Akehurst and W. B. Wright, *Journal of the American Oil Chemists Society* **48** (12), 824 (1971).
- [6].K. van Malssen, A. van Langevelde, R. Peschar and H. Schenk, *Journal of the American Oil Chemists' Society* **76** (6), 669 (1999).
- [7].I. Foubert, P. A. Vanrolleghem and K. Dewettinck, *Thermochimica Acta* **400** (1–2), 131 (2003).
- [8].J. F. Toro-Vazquez, E. Rangel-Vargas, E. Dibildox-Alvarado and M. A. Charó-Alonso, *European Journal of Lipid Science and Technology* **107** (9), 641 (2005).
- [9].D. Manning and P. Dimick, *Food Structure* **4** (2), 9 (1985).
- [10].P. Dimick and D. Manning, *Journal of the American Oil Chemists' Society* **64** (12), 1663 (1987).

- 1
2
3 [11].J. Schlichter Aronhime, S. Sarig and N. Garti, Journal of the American Oil
4 Chemists' Society **65** (7), 1140 (1988).
5 [12].S. Chaiseri and P. Dimick, Journal of the American Oil Chemists' Society **72** (12),
6 1491 (1995).
7 [13].K. Larsson, Fette, Seifen, Anstrichmittel **74** (3), 136 (1972).
8 [14].K. Larsson, in *Lipids-Molecular organisation, physical functions and technical*
9 *applications* (The Oily Press, L.T.D., Scotland, 1994), pp. 75.
10 [15].D. Cebula, D. J. McClements, M. W. Povey and P. Smith, Journal of the American
11 Oil Chemists' Society **69** (2), 130 (1992).
12 [16].R. W. Corkery, D. Rousseau, P. Smith, D. A. Pink and C. B. Hanna, Langmuir **23**
13 (13), 7241 (2007).
14 [17].D. A. Pink, C. B. Hanna, C. Sandt, A. J. MacDonald, R. MacEachern, R. Corkery
15 and D. Rousseau, The Journal of Chemical Physics **132** (5), 054502 (2010).
16 [18].A. S. Tascini, M. G. Noro, R. Chen, J. M. Seddon and F. Bresme, Physical
17 Chemistry Chemical Physics **20** (3), 1848 (2018).
18 [19].T. Arishima, N. Sagi, H. Mori and K. Sato, Journal of the American Oil Chemists
19 Society **68** (10), 710 (1991).
20 [20].F. Lavigne, C. Bourgaux and M. Ollivon, Le Journal de Physique IV **3** (C8), C8
21 (1993).
22 [21].J. Yano, K. Sato, F. Kaneko, D. M. Small and D. R. Kodali, Journal of Lipid
23 Research **40** (1), 140 (1999).
24 [22].R. Peschar, M. M. Pop, D. J. A. De Ridder, J. B. van Mechelen, R. A. J. Driessen
25 and H. Schenk, The Journal of Physical Chemistry B **108** (40), 15450 (2004).
26 [23].K. Larsson, Journal of the American Oil Chemists Society **69** (8), 835 (1992).
27 [24].P. T. Callaghan and K. W. Jolley, Chemistry and Physics of Lipids **27** (1), 49
28 (1980).
29 [25].A. K. Sum, M. J. Bidy, J. J. de Pablo and M. J. Tupy, The Journal of Physical
30 Chemistry B **107** (51), 14443 (2003).
31 [26].M. Greiner, A. M. Reilly and H. Briesen, Journal of Agricultural and Food
32 Chemistry **60** (20), 5243 (2012).
33 [27].A. Rachocki and J. Tritt-Goc, Food Chemistry **152**, 94 (2014).
34 [28].E. Stejskal and J. Tanner, J Chem Phys **42** (1965).
35 [29].K. Zick, (Bruker Corporation, Germany, 2016).
36 [30].R. Meier, R. Kahlau, D. Kruk and E. A. Rössler, The Journal of Physical
37 Chemistry A **114** (30), 7847 (2010).
38 [31].D. Kruk, R. Meier and E. A. Rössler, The Journal of Physical Chemistry B **115** (5),
39 951 (2011).
40 [32].D. Kruk, A. Korpała, A. Kubica, R. Meier, E. A. Rössler and J. Moscicki, The
41 Journal of Chemical Physics **138** (2), 024506 (2013).
42 [33].M. Flämig, M. Becher, M. Hofmann, T. Körber, B. Kresse, A. F. Privalov, L.
43 Willner, D. Kruk, F. Fujara and E. A. Rössler, The Journal of Physical Chemistry B **120**
44 (31), 7754 (2016).
45 [34].Y. L. Wang and P. S. Belton, Chemical Physics Letters **325** (1), 33 (2000).
46 [35].F. Fujara, D. Kruk and A. F. Privalov, Progress in Nuclear Magnetic Resonance
47 Spectroscopy **82**, 39 (2014).
48 [36].K. P. A. M. v. Putte and J. v. d. Enden, Journal of Physics E: Scientific Instruments
49 **6** (9), 910 (1973).
50 [37].K. Van Putte and J. Van Den Enden, Journal of the American Oil Chemists Society
51 **51** (7), 316 (1974).
52 [38].D. Kruk, R. Meier and E. A. Rössler, Physical Review E **85** (2), 020201 (2012).
53
54
55
56
57
58
59
60

- 1
2
3 [39].J. Rault, *Journal of Non-Crystalline Solids* **271** (3), 177 (2000).
4 [40].J. Brillo, A. I. Pommrich and A. Meyer, *Physical Review Letters* **107** (16), 165902
5 (2011).
6 [41].A. Takeuchi and A. Inoue, *MATERIALS TRANSACTIONS* **43** (5), 1205 (2002).
7 [42].K.-C. Chung, H.-Y. Yu and S. Ahn, *Convection Effects on PGSE-NMR Self-*
8 *Diffusion Measurements at Low Temperature: Investigation into Sources of Induced*
9 *Convective Flows.* (1970).
10 [43].W. J. Goux, L. A. Verkruyse and S. J. Saltert, *Journal of Magnetic Resonance*
11 (1969) **88** (3), 609 (1990).
12 [44].E. O. Stejskal and J. E. Tanner, *The Journal of Chemical Physics* **42** (1), 288
13 (1965).
14 [45].N. Klaas, K. P. J. Braun, R. A. d. Graaf, R. M. Dijkhuizen and M. J. Kruiskamp,
15 *NMR in Biomedicine* **14** (2), 94 (2001).
16 [46].U. o. Muenster.
17 [47].K. Nicolay, K. P. J. Braun, R. A. d. Graaf, R. M. Dijkhuizen and M. J. Kruiskamp,
18 *NMR in Biomedicine* **14** (2), 94 (2001).
19 [48].R. Kimmich and N. Fatkullin, *Progress in Nuclear Magnetic Resonance*
20 *Spectroscopy* **101**, 18 (2017).
21 [49].I. f. P. Chemie, (Universität Münster, Münster), Vol. 2018.
22 [50].E. Dibildox-Alvarado, T. Laredo, J. F. Toro-Vazquez and A. G. Marangoni,
23 *Journal of the American Oil Chemists' Society* **87** (10), 1115 (2010).
24 [51].T. Davis and P. Dimick, *Journal of the American Oil Chemists Society* **66** (10),
25 1488 (1989).
26 [52].T. Davis and P. Dimick, *Journal of the American Oil Chemists Society* **66** (10),
27 1494 (1989).
28 [53].C. Loisel, G. Keller, G. Lecq, C. Bourgaux and M. Ollivon, *Journal of the*
29 *American Oil Chemists' Society* **75** (4), 425 (1998).
30 [54].K. van Malssen, R. Peschar and H. Schenk, *Journal of the American Oil Chemists'*
31 *Society* **73** (10), 1217 (1996).
32 [55].I. Foubert, P. A. Vanrolleghem, O. Thas and K. Dewettinck, *Journal of Food*
33 *Science* **69** (9), E478 (2004).
34 [56].E. S. Lutton, *Journal of the American Chemical Society* **67** (4), 524 (1945).
35 [57].E. S. Lutton and F. L. Jackson, *Journal of the American Chemical Society* **72** (7),
36 3254 (1950).
37 [58].M. Iwahashi, Y. Kasahara, H. Matsuzawa, K. Yagi, K. Nomura and H. Terauchi, *J*
38 *Phys Chem B* **104** (2000).
39 [59].M. Iwahashi, Y. Kasahara, H. Minami, H. Matsuzawa, M. Suzuki and Y. Ozaki, *J*
40 *Oleo Sci* **51** (2002).
41 [60].I. T. Norton, C. D. Lee-Tuffnell, S. Ablett and S. M. Bociak, *Journal of the*
42 *American Oil Chemists' Society* **62** (8), 1237 (1985).
43 [61].K. van Malssen, R. Peschar and H. Schenk, *Journal of the American Oil Chemists'*
44 *Society* **73** (10), 1209 (1996).
45 [62].I. Foubert, 2003.
46 [63].B. BioSpin, (2014).
47 [64].R. Kimmich and E. Anordo, *Progress in Nuclear Magnetic Resonance*
48 *Spectroscopy* **44** (3–4), 257 (2004).
49 [65].C. I. Daniel, F. Vaca Chávez, G. Feio, C. A. M. Portugal, J. G. Crespo and P. J.
50 Sebastião, *The Journal of Physical Chemistry B* **117** (39), 11877 (2013).
51 [66].A. M. J. P., C. F. Vaca and S. P. J., *Magnetic Resonance in Chemistry* **52** (10), 540
52 (2014).
53
54
55
56
57
58
59
60

1
2
3 This article shows, to the best of our knowledge, the first self-diffusion study of cocoa butter.

4
5 This is of relevance for the confectionery industry as it is indispensable to understand the

6
7 liquid phase of cocoa butter for improving current chocolate processing conditions.

8
9 Furthermore, both fast field cycling (FFC) and pulse field stimulated echo NMR techniques

10
11 were used, validating the former as an alternative, if not superior, method for self-diffusion

12
13 measurements of triacylglycerols as it is not as sensitive to convection-related errors. Finally,

14
15 it shows that FFC NMR can be used to study fat crystallisation.
16
17
18
19
20
21
22
23
24
25
26
27
28
29
30
31
32
33
34
35
36
37
38
39
40
41
42
43
44
45
46
47
48
49
50
51
52
53
54
55
56
57
58
59
60

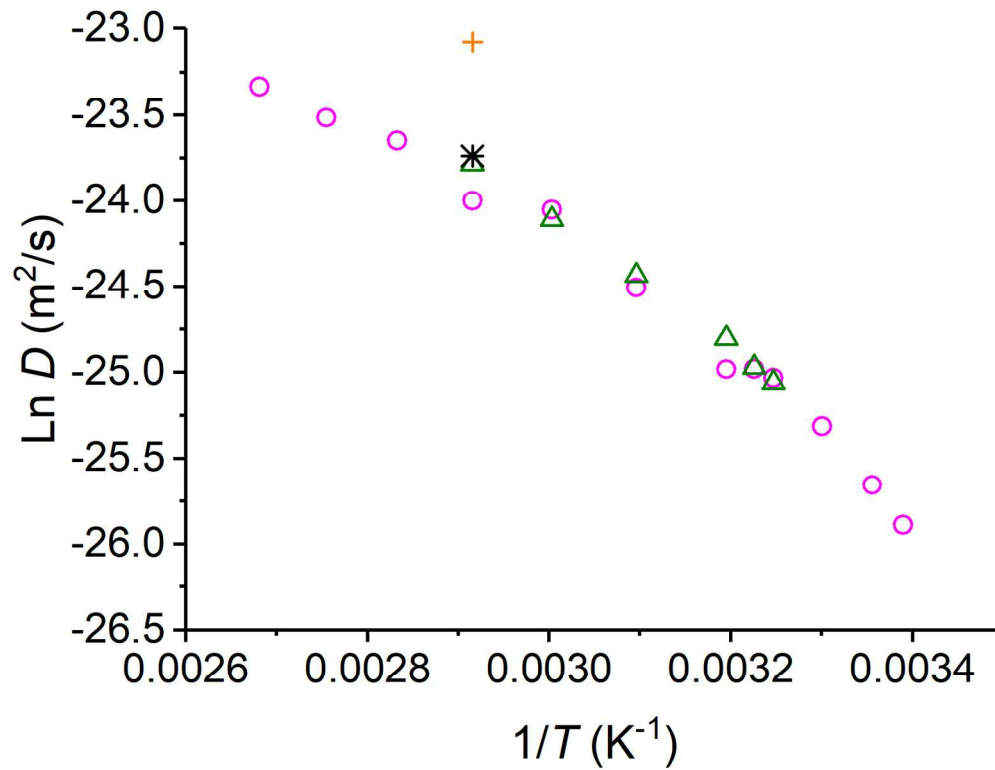


Figure 1 Diffusion coefficients of CB as determined by different techniques. The green triangles represent the values obtained from a PGSTE sequence, and the pink circles those calculated from FFC-NMR measurements upon cooling. Additionally, values for tristearin (black star) and triolein (orange cross) were taken from literature[24] for reference.

149x115mm (300 x 300 DPI)

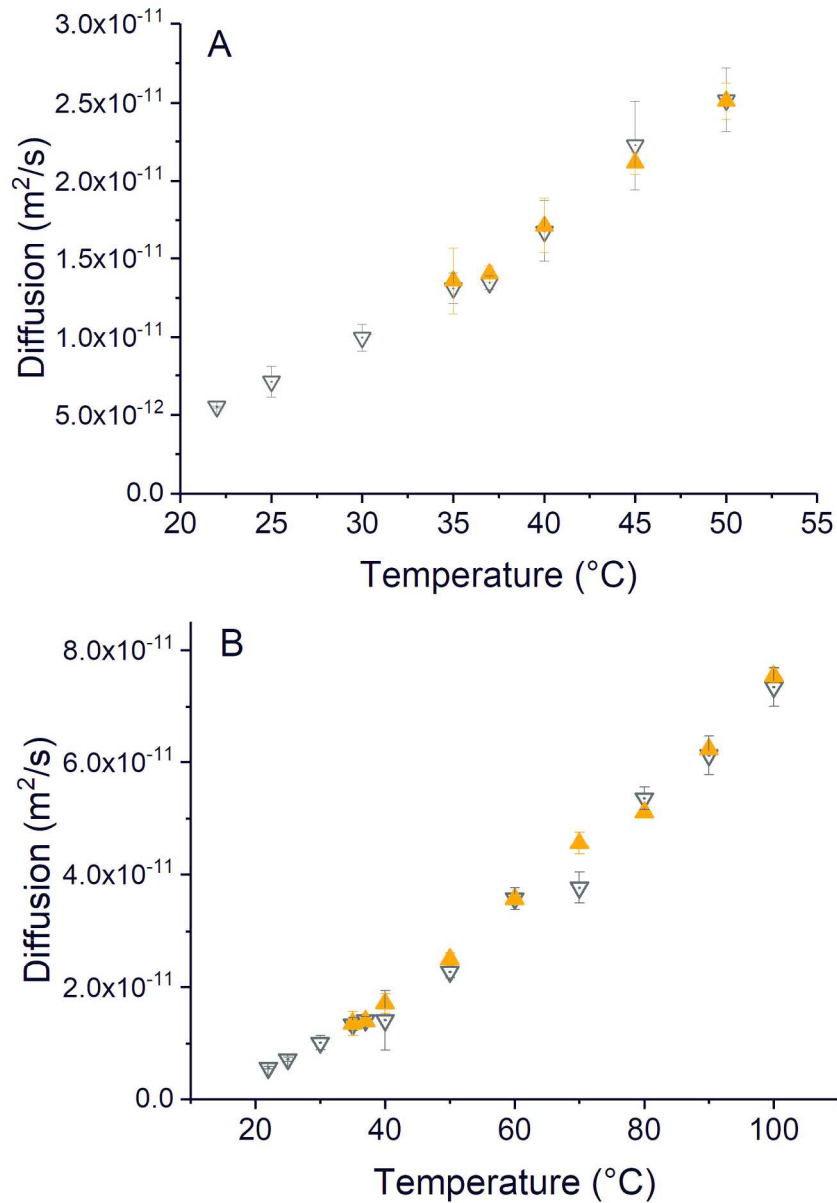


Figure 2 Diffusion coefficients calculated using FFC-NMR vs. temperature of the 50 (A) and 100 °C (B) treatments. The orange upward triangles symbolise the coefficients calculated during the heat treatment, only values from 35 °C are shown as prior to this temperature the sample was too solid for diffusion calculations. The grey downward triangles represent the values obtained on cooling the sample. Here it was possible to calculate diffusion coefficients down to 22 °C as crystallisation is not immediate. Both heating and cooling treatments were performed step-wise, allowing for at least 10 min for temperature equilibration. The error bars represent the standard deviation.

150x216mm (300 x 300 DPI)

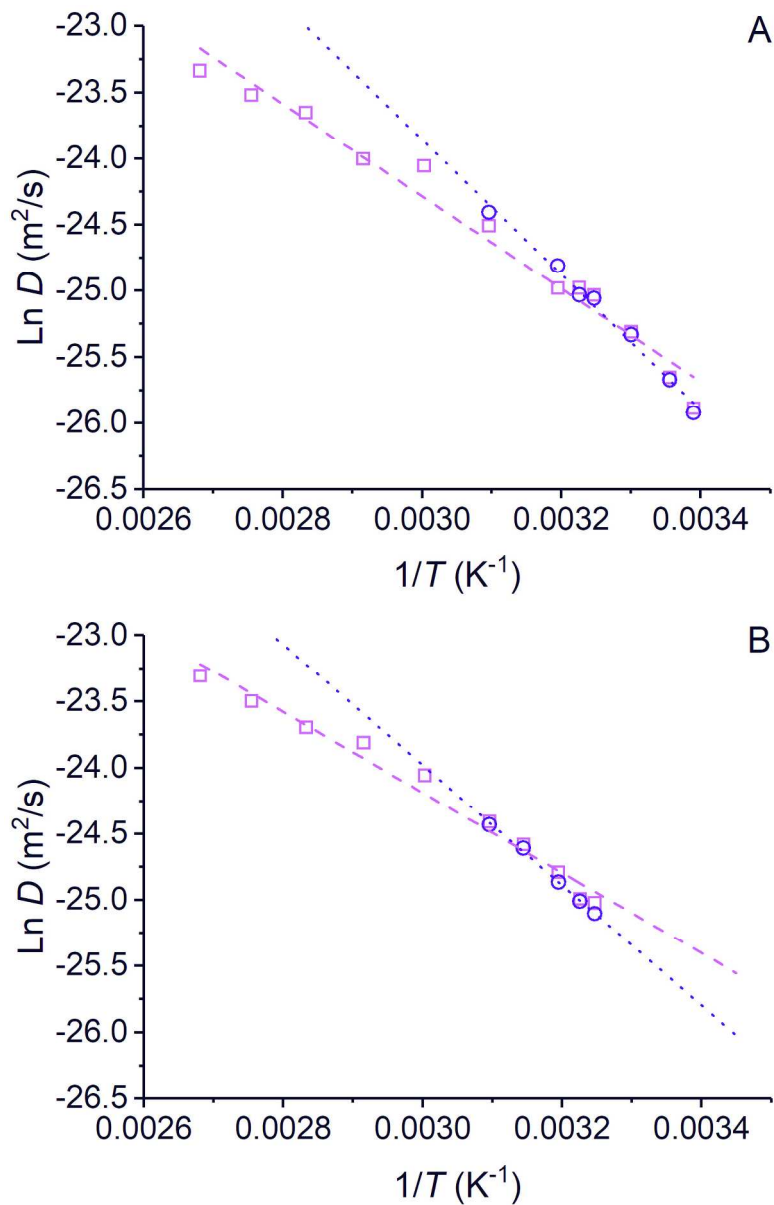


Figure 3 Arrhenius plots of diffusion coefficients calculated from the (A) cooling and (B) heating ramps for both, the 50 (blue circles) and the 100 °C (pink squares) treatments. A linear (Arrhenius) function was fitted (dotted blue and dashed pink lines, corresponding to the 50 and 100 °C treatments, respectively), from which the activation energy was estimated.

149x233mm (300 x 300 DPI)

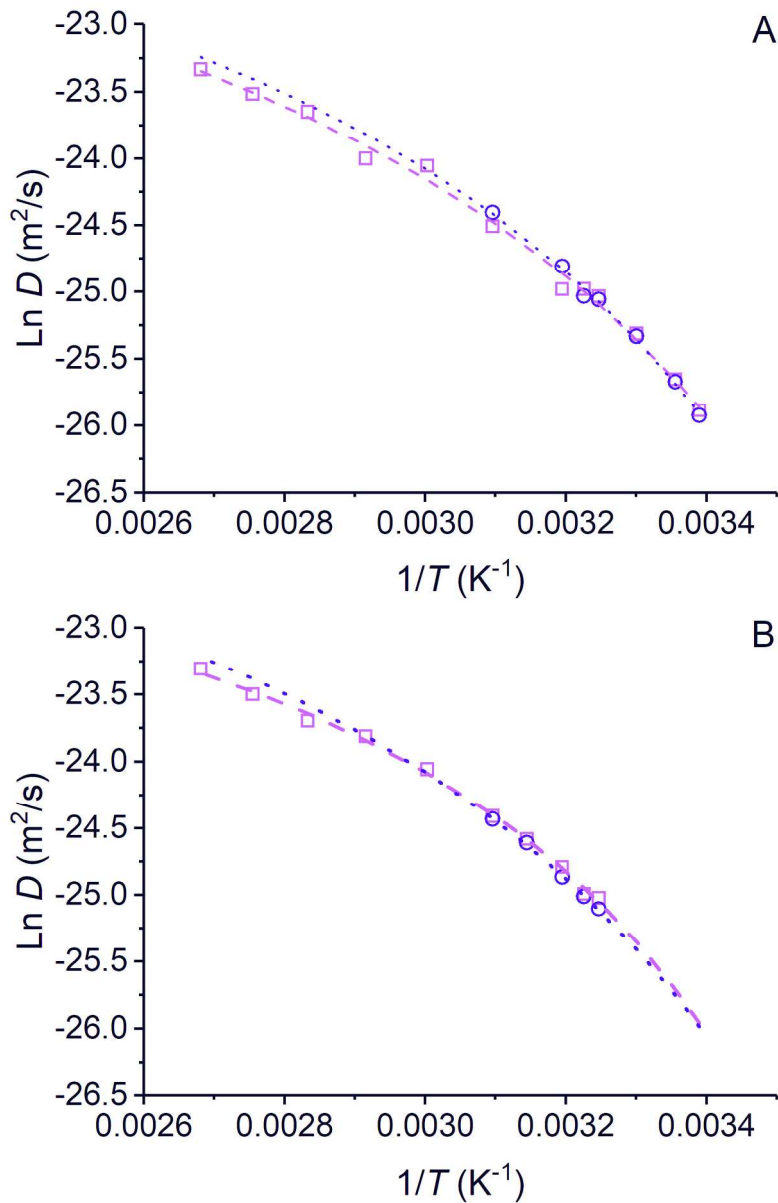


Figure 4 Temperature dependence of the self-diffusion coefficients of CB obtained from (A) cooling and (B) heating ramps for both, the 50 (blue circles) and the 100 °C (pink squares) treatments. The dotted blue and dashed pink lines, correspond to the VFT fits for the 50 and 100 °C treatments, respectively.

149x231mm (300 x 300 DPI)

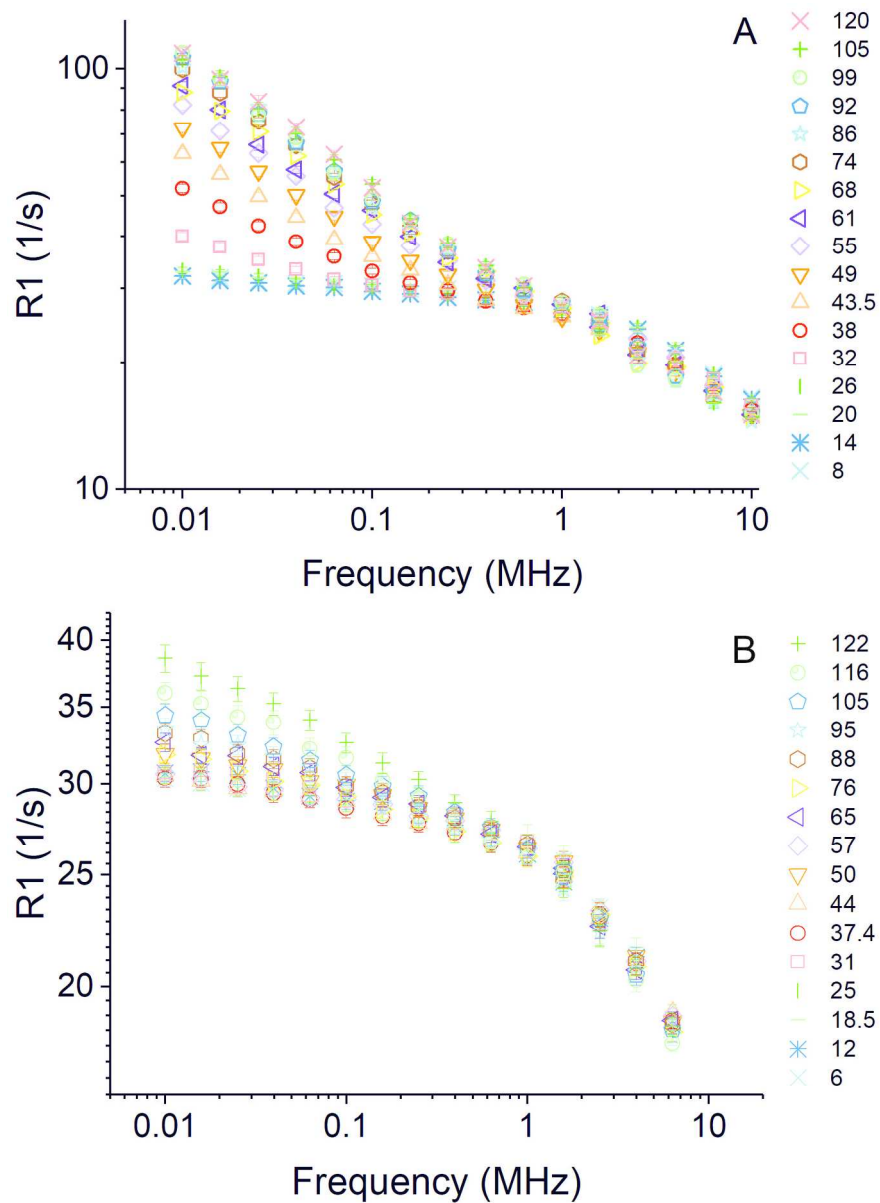
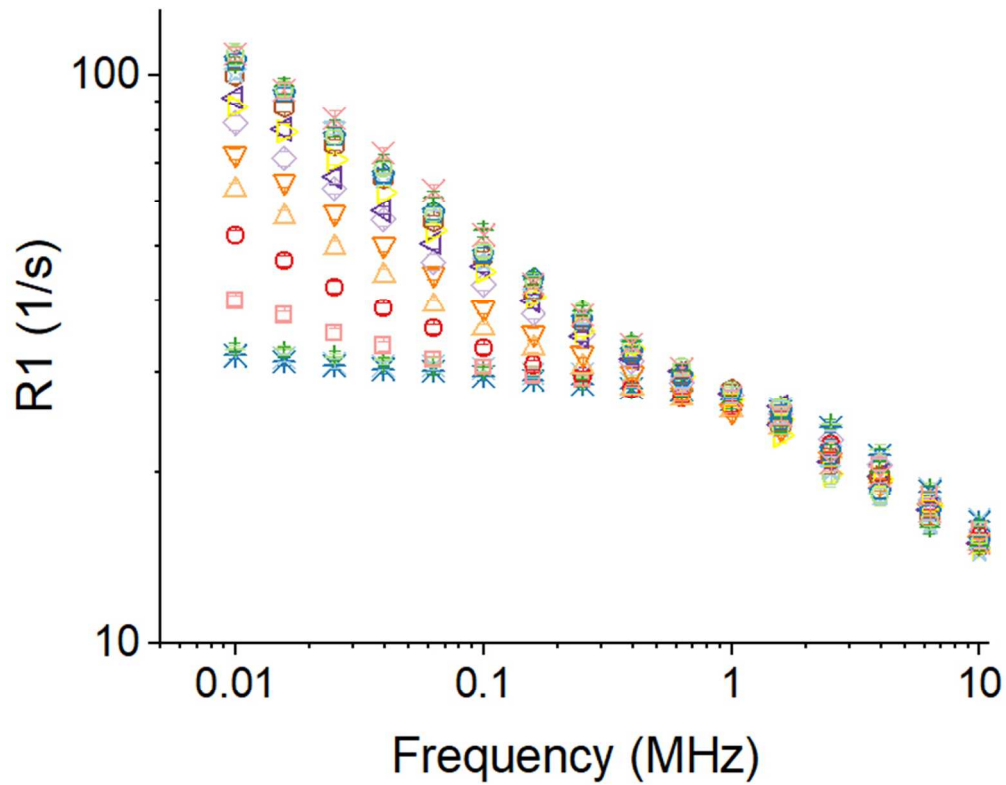


Figure 5 ^1H spin-lattice relaxation dispersion data for CB held isothermally at 22 °C for two hours. Panel A shows the measurements of CB previously heated to 50 °C and cooled down stepwise to 22 °C, whilst panel B shows the measurements of CB previously heated to 100 °C prior to stepwise cooling. In both panels, time increases from the bottom (6 min) to the top (120 min), the key on the right-hand side is indicative of the time (minutes) at which the relaxation measurements finished.

149x205mm (300 x 300 DPI)



^1H spin-lattice relaxation dispersion data for CB held isothermally at 22 °C.

64x49mm (300 x 300 DPI)